Cbl-b Is a Critical Regulator of Macrophage Activation Associated With Obesity-Induced Insulin Resistance in Mice

Tomoki Abe,[1] Katsuya Hirasaka,[1] Sachiko Kagawa,[1] Shohei Kohno,[1] Arisa Ochi,[1] Kenro Utsunomiya,[1] Atsuko Sakai,[1] Ayako Ohno,[1] Shigetada Teshima-Kondo,[1] Yuushi Okumura,[1] Motoko Oarada,[2] Yoichi Maekawa,[3] Junji Terao,[4] Edward M. Mills,[5] and Takeshi Nikawa[1]

We previously reported the potential involvement of casitas B-cell lymphoma-b (Cbl-b) in aging-related murine insulin resistance. Because obesity also induces macrophage recruitment into adipose tissue, we elucidated here the role of Cbl-b in obesity-related insulin resistance. Cbl-b$^{+/+}$ and Cbl-b$^{-/-}$ mice were fed a high-fat diet (HFD) and then examined for obesity-related changes in insulin signaling. The HFD caused recruitment of macrophages into adipose tissue and increased inflammatory reaction in Cbl-b$^{-/-}$ compared with Cbl-b$^{+/+}$ mice. Peritoneal macrophages from Cbl-b$^{-/-}$ mice and Cbl-b–overexpressing RAW264.7 macrophages were used to examine the direct effect of saturated fatty acids (FAs) on macrophage activation. In macrophages, Cbl-b suppressed saturated FA-induced Toll-like receptor 4 (TLR4) signaling by ubiquitination and degradation of TLR4. The physiological role of Cbl-b in vivo was also examined by bone marrow transplantation and Eritoran, a TLR4 antagonist. Hematopoietic cell-specific depletion of the Cbl-b gene induced disturbed responses on insulin and glucose tolerance tests. Blockade of TLR4 signaling by Eritoran reduced fasting blood glucose and serum interleukin-6 levels in obese Cbl-b$^{-/-}$ mice. These results suggest that Cbl-b deficiency could exaggerate HFD-induced insulin resistance through saturated FA-mediated macrophage activation. Therefore, inhibition of TLR4 signaling is an attractive therapeutic strategy for treatment of obesity-related insulin resistance. ***Diabetes*** **62:1957–1969, 2013**

Obesity is sometimes associated with a chronic inflammatory state, insulin resistance, and type 2 diabetes (1,2). One feature of obesity-induced inflammation is the recruitment of macrophages into white adipose tissue (WAT). These activated macrophages secrete proinflammatory cytokines, such as tumor necrosis factor-α (TNF-α), interleukin-6 (IL-6), and monocyte chemoattractant protein-1 (MCP-1), and induce localized insulin resistance (3–5). Furthermore, the cytokines, adipokines, and free fatty acids (FAs) released from the WAT also act on the endocrine system, liver, and muscles and may reduce insulin sensitivity within these organs (6).

Casitas B-cell lymphoma-b (Cbl-b) is a unique ubiquitin ligase involved in the maturation and activation of macrophages and T lymphocytes (7,8). Expression of Cbl-b is upregulated with macrophage differentiation of the HL60 and U937 cell lines (7). We have already reported that recruitment of macrophages into the WAT is markedly augmented in elderly Cbl-b–deficient (Cbl-b$^{-/-}$) mice and that their accumulation is associated with systemic insulin resistance and glucose intolerance (9). The current study demonstrated that a high-fat diet (HFD) induced accumulation of macrophages in WAT and insulin resistance in Cbl-b$^{-/-}$ mice at an earlier stage than in Cbl-b$^{-/-}$ mice fed a normal diet (ND). Feeding an HFD for 5 weeks induces macrophage accumulation and insulin resistance even in young Cbl-b$^{-/-}$ mice, whereas at least a 20-week period is often required to induce a similar phenomenon in Cbl-b$^{-/-}$ mice fed an ND (9).

Free FAs, especially saturated FAs, induce activation of macrophages and aggravate the inflammatory process in WAT (6,10,11). Saturated FAs can activate Toll-like receptor 4 (TLR4), which is a receptor for lipopolysaccharides (LPS), and trigger the activation of its adaptor protein myeloid differentiation factor 88 (MyD88) and a downstream signaling cascade, leading to upregulation of cytokine expression through the nuclear factor-κB (NF-κB) inflammatory signaling pathway (12–14). Recent experiments showed that Cbl-b binds to TLR4 and MyD88 in neutrophils and TLR4-overexpressing HEK293 cells (15). We therefore hypothesized that Cbl-b is a critical regulator of saturated FA-induced cytokine expression in macrophages and neutrophils.

The aim of this study was to elucidate the pathophysiological role of Cbl-b in the mechanism of macrophage activation by saturated FAs. The results showed that Cbl-b deficiency was associated with recruitment of macrophages into the WAT at the early stages of HFD-induced obesity. Cbl-b is an important molecule in diet-induced obesity and insulin resistance, especially through the activation of macrophages.

RESEARCH DESIGN AND METHODS

Animals, obesity induction, and TLR4 antagonist treatment. Cbl-b$^{-/-}$ mice were provided by the National Institutes of Health (Rockville, MD) and were backcrossed more than eight times into the C57BL/6 strain (16,17). We used C57BL/6 mice (Japan SLC, Shizuoka, Japan) as wild-type (Cbl-b$^{+/+}$) mice.

Eight-week-old Cbl-b$^{+/+}$ and Cbl-b$^{-/-}$ mice were divided into two groups; the first group was fed an ND (10% of the calories as fat), whereas the mice of the second group were fed an HFD (60% of the calories as fat). Eritoran is an analog of LPS that antagonizes its activity by binding to the TLR4–MD-2 complex (18).

From the [1]Department of Nutritional Physiology, Institute of Health Biosciences, The University of Tokushima Graduate School, Tokushima, Japan; the [2]Medical Mycology Research Center, The University of Chiba, Chiba, Japan; the [3]Department of Immunology and Parasitology, Institute of Health Biosciences, The University of Tokushima Graduate School, Tokushima, Japan; the [4]Department of Food Science, Institute of Health Biosciences, The University of Tokushima Graduate School, Tokushima, Japan; and [5]Pharmacology/Toxicology, College of Pharmacy, University of Texas at Austin, Austin, Texas.

Corresponding author: Takeshi Nikawa, nikawa@nutr.med.tokushima-u.ac.jp.

Received 25 May 2012 and accepted 17 January 2013.

DOI: 10.2337/db12-0677

This article contains Supplementary Data online at http://diabetes.diabetesjournals.org/lookup/suppl/doi:10.2337/db12-0677/-/DC1.

Eritoran and its placebo were a gift from Eisai Research Institute (Andover, MA). After being fed the HFD for 5 weeks, Cbl-b$^{+/+}$ and Cbl-b$^{-/-}$ mice were injected intraperitoneally with Eritoran (4 mg/kg body weight) or placebo, three times every 24 h. The experimental protocols described in this study were approved by the Tokushima University Ethics Review Committee for Animal Experimentation.

Isolation of stromal vascular fraction and flow cytometry. Isolation of stromal vascular (SV) fraction and flow cytometry was conducted as described in detail previously (9). To determine cell-surface TLR4 protein levels in peritoneal macrophages from Cbl-b$^{+/+}$ (n = 3) and Cbl-b$^{-/-}$ mice (n = 3), these macrophages were incubated with fluorescein isothiocyanate isomer-I–labeled anti-F4/80 (eBioscience, San Diego, CA) and phycoerythrin-labeled anti-TLR4 (eBioscience) antibody.

Bone marrow transplantation. Bone marrow transplantation (BMT) was conducted as described previously (19). Bone marrow cells (5×10^6 cells) were harvested from Cbl-b$^{+/+}$ and Cbl-b$^{-/-}$ mice by flushing with PBS. The recipient 5-week-old C57BL/6 mice were lethally irradiated at a dose of 7 Gy with an irradiator (MBR-1520R-3, Hitachi, Tokyo). Bone marrow cells were then injected in the retro-orbital venous plexus of the recipient mice. The mice were fed the HFD 3 weeks later. We confirmed the efficiency of this BMT technique by measuring the ratio of bone marrow cells derived from green fluorescence protein (GFP) transgenic mice to the bone marrow of wild-type mice. The proportion of GFP-positive cells at 8 weeks after BMT, as analyzed by flow cytometry, was 91.7 ± 3.3% relative to the total bone marrow cells in recipient mice.

Histological analysis. Paraffin-embedded sections of epididymal WAT (6-μm thickness) were prepared and stained by standard techniques for histological analysis (9).

Cell culture, transfection, and treatment. The RAW264.7 macrophage cell line (ATCC, Rockville, MD) was maintained in Dulbecco's modified Eagle's medium (DMEM) containing 10% FBS, 100 U/mL penicillin, and 100 μg/mL streptomycin at 37°C under a 5% carbon dioxide-95% air mixture. HEK293-mTLR4/MD2-CD14 (HEK293/TLR4) cells (InvivoGen, San Diego, CA), an isolated clone of HEK293 cells stably transfected with mouse TLR4, MD2, and CD14 genes, were maintained with DMEM containing 10 μg/mL blasticidin (InvivoGen) and 50 μg/mL high-purity hygromycin B (InvivoGen).

RAW264.7 macrophages and HEK293 cells were transfected with plasmid vectors containing the indicated genes by using a FuGENE HD lipofection reagent (Roche Diagnostics, Tokyo, Japan). The expression plasmids used in this study were prepared as described previously (17): pcDNA3.1-TLR4-V5, pcDNA3.1-MyD88-Myc, pCEFL-Cbl-b–hemagglutinin (HA), and pcDNA3.1-FLAG-ubiquitin. Mock vector, such as pCEFL, was used as the control vector.

Peritoneal macrophages, RAW264.7 cells, and HEK293 cells were treated with 400 μmol/L palmitate (C16:0) conjugated with BSA. Peritoneal macrophages were also pretreated with chemical inhibitors or a neutralizing antibody 1 or 2 h before palmitate treatment, respectively: 500 nmol/L inhibitor of NF-κB kinase (IKK) 2-IV inhibitor (Calbiochem) as NF-κB inhibitor, 25 μmol/L SP600125 (Calbiochem, San Diego, CA) as Jun *N*-terminal kinase (JNK) inhibitor, and 18 μg/mL of anti-TLR4/MD-2 IgG (eBioscience, San Diego, CA). We checked the efficacy of this neutralizing antibody against LPS-mediated IL-6 expression in peritoneal macrophages (Supplementary Fig. 1).

Immunoblotting and immunoprecipitation. Immunoblot and immunoprecipitation analyses were performed as described previously (20). The following antibodies were used: anti–β-actin (Oncogene Research Products, San Diego, CA), anti-Akt1 (PharMingen International, Tokyo), antiphospho-Akt, antiphospho-inhibitor of NF-κB (IκB)-α, anti-JNK, antiphospho-JNK, anti-Myc (Cell Signaling Technology, Beverly, MA), anti-HA.11 (BabCo, Richmond, CA), anti-V5 (Invitrogen), anti–Cbl-b (Santa Cruz Biotechnology, Santa Cruz, CA), anti-FLAG M2 (Sigma), anti-MyD88 (Biovision, Milpitas, CA), anti-TRIF (Novus Biologicals, Littleton, CO), and anti–IκB-α (Upstate Biotechnology, Lake Placid, NY).

Real-time RT-PCR. Real-time RT-PCR was performed with SYBR green dye using the ABI 7300 real-time RT-PCR system (Applied Biosystems, Foster City, CA), as described previously (21). The oligonucleotide primers used for amplification are listed in Supplementary Table 1.

Measurement of other biochemical parameters. The protein concentration was determined by bicinchoninic acid assay, as described previously (22). Serum concentrations of triglyceride and nonesterified FAs were measured with respective kits, as described previously (23,24). The concentrations of serum insulin, leptin, adiponectin, and MCP-1 were determined by using enzyme-linked immunosorbent assay (ELISA) kits (Morinaga Institute, Tokyo; Otsuka, Tokyo, Japan and R&D Systems, Minneapolis, MN, respectively) (9). An intraperitoneal insulin tolerance test (ITT) and a glucose tolerance test (GTT) were performed after a 12-h fast, using the method described previously (25).

Statistical analysis. Data are expressed as means ± SD (n = 3–10). Differences between two groups were assessed with Duncan's multiple range test, and differences among groups were evaluated by ANOVA. All statistical analysis was conducted using SPSS 6.1 software (SPSS Japan, Tokyo, Japan). Differences were considered significant at $P < 0.05$.

RESULTS

Metabolic parameters in Cbl-b$^{-/-}$ mice fed the HFD. To examine the effects of Cbl-b deficiency on metabolic features of diet-induced obese mice, we compared food intake, wet weights of various tissues, and serum metabolic parameters in Cbl-b$^{+/+}$ and Cbl-b$^{-/-}$ mice fed the ND or HFD for 5 weeks (Table 1). The concentrations of serum leptin and nonesterified FAs in Cbl-b$^{-/-}$ mice were significantly higher than those in Cbl-b$^{+/+}$ mice fed the ND for 5 weeks. Body weight gain after being fed the HFD was higher in Cbl-b$^{-/-}$ mice than in Cbl-b$^{+/+}$ mice, although the food intake was smaller in Cbl-b$^{-/-}$ mice than in Cbl-b$^{+/+}$ mice. Consistent with this finding, serum leptin levels were higher in Cbl-b$^{-/-}$ mice fed the HFD than in Cbl-b$^{+/+}$ mice fed the same diet. In contrast, serum adiponectin levels were lower in Cbl-b$^{-/-}$ mice fed the HFD. The serum levels of nonesterified FAs and triglycerides were higher in

TABLE 1
Metabolic parameters in Cbl-b$^{-/-}$ mice or BMT mice fed the HFD

	ND		HFD			
	Cbl-b$^{+/+}$	Cbl-b$^{-/-}$	Cbl-b$^{+/+}$	Cbl-b$^{-/-}$	Cbl-b$^{+/+}$ BMT	Cbl-b$^{-/-}$ BMT
Food intake (g/day)	4.3 ± 0.3	3.9 ± 0.5	3.7 ± 1.2	2.1 ± 0.3*#	3.2 ± 0.7	2.9 ± 0.5
Body weight (g)	27.4 ± 0.5	26.0 ± 2.3	29.7 ± 1.7#	33.0 ± 2.2*#	39.48 ± 0.9	34.50 ± 3.0
Epididymal fat weight % (g/body weight)	0.71 ± 0.27	0.63 ± 0.23	0.92 ± 0.23	2.76 ± 0.58*#	4.06 ± 0.26	3.47 ± 0.64
Gastrocnemius muscle weight % (g/body weight)	0.58 ± 0.07	0.53 ± 0.04	0.59 ± 0.12	0.42 ± 0.02*	0.38 ± 0.03	0.44 ± 0.07
Liver weight % (g/body weight)	4.30 ± 0.67	4.06 ± 0.37	3.90 ± 0.50	3.79 ± 0.70	2.92 ± 0.36	3.02 ± 0.22
Insulin (pmol/L)	40.0 ± 5.3	42.1 ± 6.2	52.6 ± 10.0	59.0 ± 22.2	46.07 ± 13.2	53.8 ± 13.4
Leptin (ng/mL)	Not detected	3.91 ± 3.34*	1.95 ± 2.24	23.17 ± 3.61*#	12.61 ± 2.19	13.56 ± 5.24
Adiponectin (μg/mL)	25.2 ± 4.7	21.0 ± 4.1	24.1 ± 4.4	18.9 ± 2.3*	34.8 ± 3.4	31.77 ± 2.2
Nonesterified fatty acid (mmol/L)	0.30 ± 0.02	0.40 ± 0.04*	0.27 ± 0.05	1.01 ± 0.38*#	1.03 ± 0.08	0.96 ± 0.19
Triglycerides (mmol/L)	1.46 ± 0.12	1.49 ± 0.27	1.30 ± 0.18	2.59 ± 0.55*#	2.38 ± 0.08	2.64 ± 0.45

Data are mean ± SD (n = 5–6). Cbl-b$^{+/+}$ and Cbl-b$^{-/-}$ mice (8 weeks old) were fed the ND or HFD for 5 weeks. Cbl-b$^{+/+}$ BMT and Cbl-b$^{-/-}$ BMT mice (8 weeks old), prepared as described in RESEARCH DESIGN AND METHODS, were also fed the HFD for 24 weeks. Blood and tissues were collected from mice that were fed the experimental diet. Biochemical markers and tissue wet-weight were measured. *$P < 0.05$ and #$P < 0.05$ compared with Cbl-b$^{+/+}$ mice on the same diet and mice of the same genotype fed the ND, respectively.

Cbl-b$^{-/-}$ mice fed the HFD than those in Cbl-b$^{+/+}$ mice fed the same diet. These findings indicate that even under ND conditions, Cbl-b$^{-/-}$ mice had disordered lipid metabolism. The HFD also induced abnormalities of lipid metabolism in Cbl-b$^{-/-}$ mice.

Recruitment of macrophages into adipose tissue in Cbl-b$^{-/-}$ mice with early obesity. Histochemical analysis showed marked recruitment of mononuclear cells into the WAT in Cbl-b$^{-/-}$ mice fed the HFD for 5 and 18 weeks compared with Cbl-b$^{+/+}$ mice under the same conditions (Fig. 1*A*). Mean adipocyte size in the WAT of Cbl-b$^{-/-}$ mice fed the HFD for 5 weeks was increased compared with that of Cbl-b$^{+/+}$ mice (Fig. 1*B*). Immunohistochemistry for F4/80, a marker of macrophages, indicated that these mononucleated cells were mainly macrophages (Fig. 1*C*). The number of crown-like structure (CLS) was increased in the WAT of Cbl-b$^{-/-}$ mice fed the HFD for 5 weeks compared with Cbl-b$^{+/+}$ mice fed same diet (Fig. 1*C*). The expression of F4/80 was increased about twofold in the WAT of Cbl-b$^{-/-}$ mice compared with Cbl-b$^{+/+}$ mice (Fig. 1*D*), in agreement with the results of immunohistochemical analysis (Fig. 1*C*). To further quantify macrophages in WAT, we performed flow cytometric analysis using cells in the adipose SV fraction obtained from Cbl-b$^{+/+}$ and Cbl-b$^{-/-}$ mice fed the HFD for 5 weeks. Cbl-b deficiency was associated with an increased population of F4/80^{+}-CD11b^{+} macrophages in the SV fraction (Fig. 1*E*). We also measured the expression of inflammatory cytokines and chemokines in the WAT of obese Cbl-b$^{-/-}$ mice. The HFD for 5 weeks increased the expression levels of IL-6 and TNF-α by ~1.5-fold in Cbl-b$^{-/-}$ mice compared with Cbl-b$^{+/+}$ mice (Fig. 1*F*). The WAT of obese Cbl-b$^{-/-}$ mice contained lower levels of adiponectin and higher levels of leptin compared with Cbl-b$^{+/+}$ mice (Fig. 1*G*). The expression and serum levels of MCP-1 were higher in obese Cbl-b$^{-/-}$ mice than in Cbl-b$^{+/+}$ mice (Fig. 1*H* and *I*).

Disturbance of insulin signaling in insulin-sensitive organs of Cbl-b$^{-/-}$ mice. Phosphorylation of Akt after insulin injection was attenuated in WAT, skeletal muscle, and liver of obese Cbl-b$^{-/-}$ mice, although insulin-induced Akt phosphorylation was noted in the respective organs of Cbl-b$^{+/+}$ mice (Fig. 2*A*). We reported previously that elderly (>30-week-old) Cbl-b$^{-/-}$ mice fed the ND developed

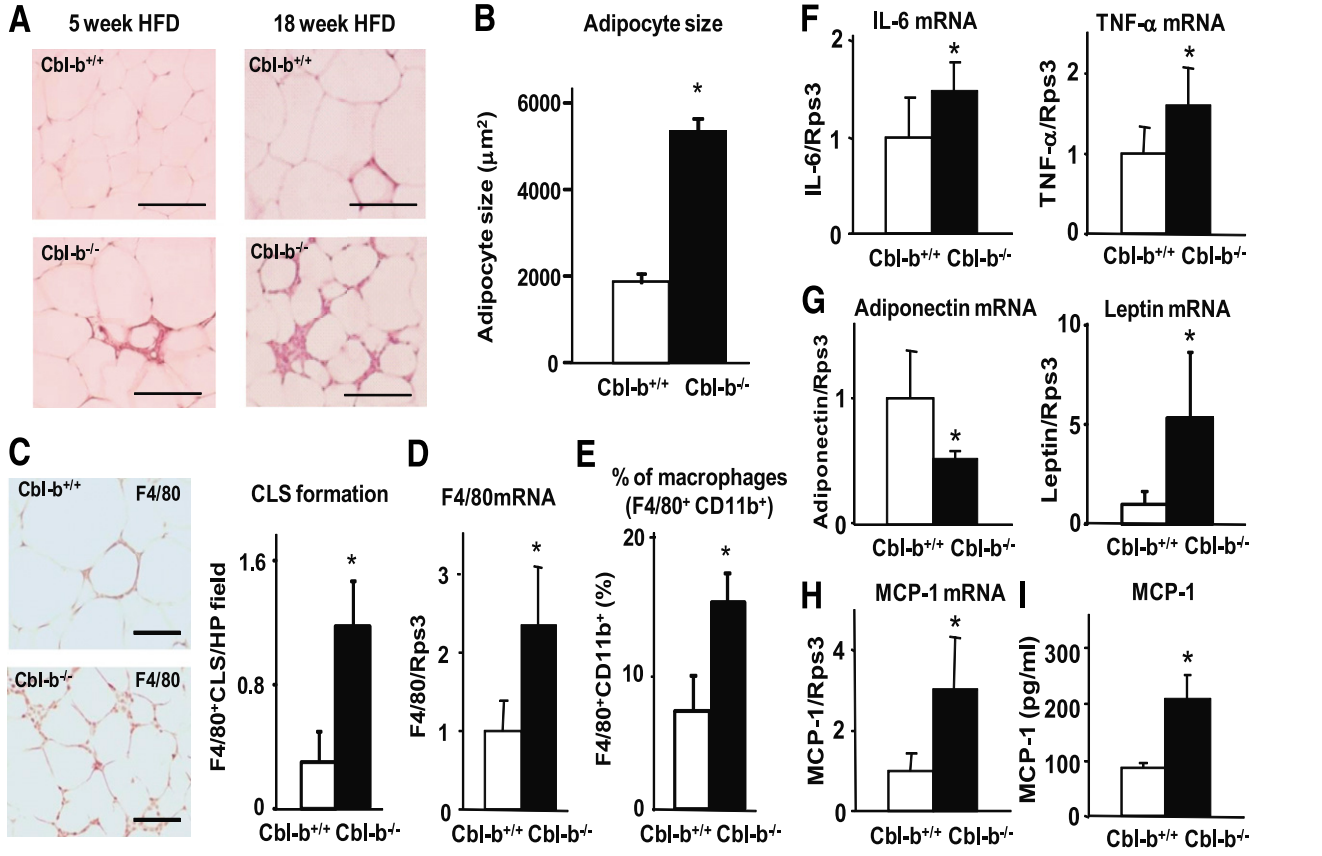

FIG. 1. Early recruitment of macrophages into epididymal WAT in Cbl-b$^{-/-}$ mice fed the HFD. *A*: The WAT of Cbl-b$^{+/+}$ (n = 4) and Cbl-b$^{-/-}$ mice (n = 4) fed the HFD for 5 or 18 weeks was stained with hematoxylin and eosin. Scale bar = 100 μm. *B*: Mean adipocyte cross-sectional area (μm^2) was assessed on *A*. Data are mean ± SD (n = 4). *P < 0.05 compared with Cbl-b$^{+/+}$ mice. *C*: The slides of WAT from Cbl-b$^{+/+}$ and Cbl-b$^{-/-}$ mice fed the HFD for 18 weeks, prepared as described above, were subjected to immunohistochemistry for F4/80, a macrophage marker. Immunoreactivity for F4/80 was visualized by diaminobenzidine staining. The number of CLS was counted in 15 high-power (HP) fields in seven slides per mice. Data are mean ± SD (Cbl-b$^{+/+}$, n = 3; Cbl-b$^{-/-}$, n = 3). *P < 0.05 compared with Cbl-b$^{+/+}$ mice. Scale bar = 100 μm. *D*: Real-time RT-PCR analysis of F4/80 expression in WAT from Cbl-b$^{+/+}$ and Cbl-b$^{-/-}$ mice fed the HFD for 5 weeks. The level of transcript was normalized to that in Cbl-b$^{+/+}$ mice. Data are mean ± SD (Cbl-b$^{+/+}$, n = 5; Cbl-b$^{-/-}$, n = 4). *P < 0.05 compared with Cbl-b$^{+/+}$ mice. *E*: Proportions of F4/80 and CD11b double-positive cells to total cells in SV fractions from WAT of Cbl-b$^{+/+}$ and Cbl-b$^{-/-}$ mice fed the HFD for 5 weeks analyzed by flow cytometry. Data are mean ± SD (Cbl-b$^{+/+}$, n = 4; Cbl-b$^{-/-}$, n = 3). *P < 0.05 compared with Cbl-b$^{+/+}$ mice. Expression of cytokines and chemokines in WAT of Cbl-b$^{+/+}$ and Cbl-b$^{-/-}$ and mice fed the HFD for 5 weeks. Real-time RT-PCR analysis of the expression levels of IL-6 and TNF-α (*F*), adiponectin and leptin (*G*), and MCP-1 transcripts (*H*) in WAT of Cbl-b$^{+/+}$ and Cbl-b$^{-/-}$ mice fed the HFD for 5 weeks. The level of each transcript was normalized to that in Cbl-b$^{+/+}$ mice. Data are mean ± SD (Cbl-b$^{+/+}$, n = 5; Cbl-b$^{-/-}$, n = 4). *I*: Serum concentrations of MCP-1 in Cbl-b$^{+/+}$ and Cbl-b$^{-/-}$ mice fed the HFD for 5 weeks measured by ELISA. Data are mean ± SD (Cbl-b$^{+/+}$, n = 3; Cbl-b$^{-/-}$, n = 4). *P < 0.05 compared with Cbl-b$^{+/+}$ mice.

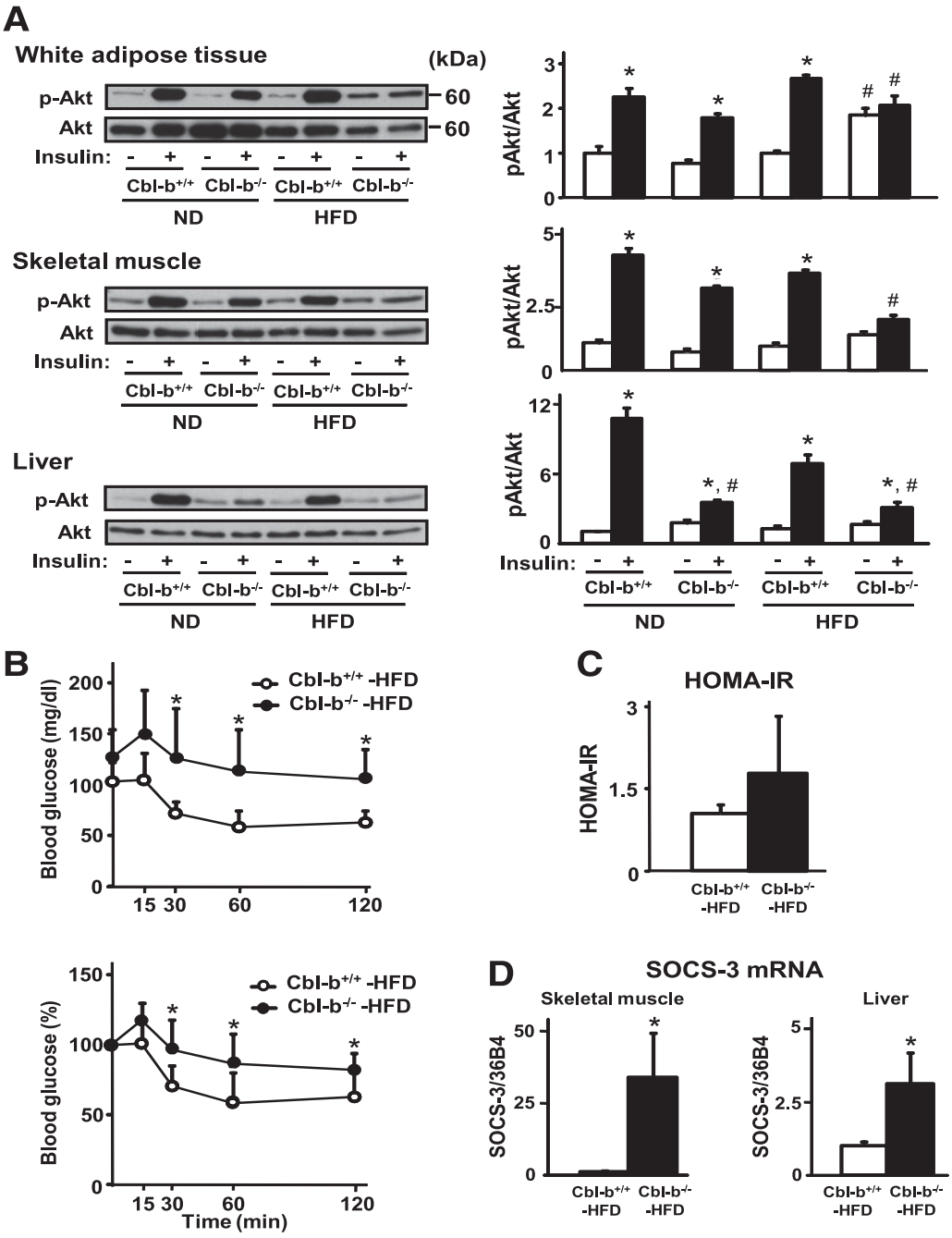

FIG. 2. Disturbance of insulin signaling in insulin-sensitive organs of Cbl-b$^{-/-}$ mice. Cbl-b$^{+/+}$ and Cbl-b$^{-/-}$ mice fed the ND or HFD for 5 weeks were fasted for 12 h and then injected intraperitoneally with 0.75 mU/g body weight of insulin or vehicle (PBS). WAT, gastrocnemius skeletal muscle, and liver were isolated after 15 min of injection. *A*: Phosphorylation of Akt as insulin signal molecule was assessed by immunoblotting. Immunoblots from three independent experiments were quantified by densitometry using ImageJ imaging software (http://imagej.nih.gov). Data are densitometric ratio of phosphorylated Akt to total Akt and are mean ± SD values of three mice. *$P < 0.05$ and #$P < 0.05$ compared with PBS and Cbl-b$^{+/+}$ mice fed the same diet, respectively. *B*: After injection of insulin, the blood glucose concentration was measured at the indicated time intervals. Data are mean ± SD (Cbl-b$^{+/+}$, $n = 6$; Cbl-b$^{-/-}$, $n = 7$). *$P < 0.05$ compared with Cbl-b$^{+/+}$ mice. *C*: HOMA-IR was calculated by the following equation: HOMA-IR = fasting blood glucose (mg/dL) × fasting serum insulin (μU/mL)/405. Data are mean ± SD (Cbl-b$^{+/+}$, $n = 5$; Cbl-b$^{-/-}$, $n = 6$). *D*: SOCS-3 mRNA levels in skeletal muscle and liver of Cbl-b$^{+/+}$ and Cbl-b$^{-/-}$ mice fed the HFD for 5 weeks, estimated by real-time RT-PCR. Data are mean ± SD ($n = 3$). *$P < 0.05$ compared with Cbl-b$^{+/+}$ mice.

impaired insulin tolerance compared with normal insulin sensitivity in young (10-week-old) Cbl-b$^{-/-}$ mice fed the same diet (9). Consistent with the result of Akt phosphorylation, a significant impairment of insulin sensitivity was noted in young (12-week-old) obese Cbl-b$^{-/-}$ mice compared with their Cbl-b$^{+/+}$ counterparts (Fig. 2*B* and *C*). In addition, the expression of suppressor of cytokine signaling-3 (SOCS-3), which interferes with insulin signal transduction (26), was increased in skeletal muscle and liver of Cbl-b$^{-/-}$ mice fed the HFD compared with Cbl-b$^{+/+}$ mice fed the same diet (Fig. 2*D*). There were no differences in these parameters between Cbl-b$^{+/+}$ and Cbl-b$^{-/-}$ mice fed the ND (data not shown). Because the expression of SOCS-3 is upregulated by proinflammatory cytokines, such as IL-6 (26), the easier induction of obesity in Cbl-b$^{-/-}$ mice may explain systemic insulin resistance via SOCS-3 expression.

Saturated FA-mediated activation of NF-κB and JNK signaling in Cbl-b–deficient macrophages. Palmitate treatment significantly reduced the levels of Cbl-b mRNA and its protein in peritoneal Cbl-b$^{+/+}$ macrophages and RAW264.7 cells, respectively (Supplementary Fig. 2), suggesting that dietary lipid can inactivate Cbl-b–mediated signaling in macrophages. To elucidate the role of Cbl-b in macrophage activation, Cbl-b$^{-/-}$ macrophages were treated with saturated FA. Palmitate upregulated IL-6 expression in Cbl-b$^{+/+}$ macrophages, and Cbl-b gene deficiency further enhanced palmitate-mediated IL-6 expression in macrophages (Fig. 3*A*). In addition, treatment with this saturated FA enhanced IL-6 expression in macrophages but not in lymphocytes or neutrophils (Supplementary Fig. 3). We also examined the response of NF-κB and JNK signaling pathways, which are essential for IL-6 expression (27), in peritoneal Cbl-b$^{+/+}$ and Cbl-b$^{-/-}$ macrophages treated with palmitate. Consistent with previous reports (13,28), incubation of peritoneal Cbl-b$^{+/+}$ macrophages with palmitate stimulated IκB phosphorylation (Fig. 3*B*). The palmitate-stimulated IκB phosphorylation was significantly enhanced in peritoneal Cbl-b$^{-/-}$ macrophages (Fig. 3*B*). Interestingly, palmitate gradually degraded total IκB in Cbl-b$^{-/-}$ macrophages (Fig. 3*B*). Phosphorylation of the ^{32}Ser residue of IκB causes its degradation (29). This finding supports the enhanced phosphorylation of IκB in Cbl-b$^{-/-}$ macrophages. Moreover, the palmitate-stimulated JNK phosphorylation, as well as IκB phosphorylation, was significantly enhanced in peritoneal Cbl-b$^{-/-}$ macrophages (Fig. 3*C*). These findings suggest that Cbl-b gene deficiency is associated with saturated FA-mediated activation of NF-κB and JNK signaling in macrophages. To elucidate this hypothesis, we also examined the effects of chemical inhibition of both pathways on IL-6 expression in peritoneal macrophages. Consistently, both NF-κB and JNK inhibitors significantly suppressed palmitate-induced IL-6 expression in Cbl-b$^{-/-}$ macrophages (Fig. 3*D*).

To determine whether Cbl-b is associated with the TLR4 signaling, peritoneal macrophages were treated with a neutralizing anti–TLR4/MD-2 IgG, which is known to suppress LPS-induced cytokine production (30). Blockade of TLR4 signaling with the neutralizing antibody suppressed the enhancement of palmitate-induced IL-6 expression observed in Cbl-b$^{-/-}$ macrophages (Fig. 3*E*). This result suggests that TLR4 expression in Cbl-b$^{-/-}$ macrophages was higher than that in Cbl-b$^{+/+}$ macrophages, so that deficiency of the Cbl-b gene further enhanced the palmitate-enhanced IL-6 expression in macrophages. To dismiss this hypothesis, we examined palmitate-induced TLR4 expression in Cbl-b$^{-/-}$ macrophages. Throughout the experiment (until 16 h after treatment), there was no significant change in TLR4 expression in Cbl-b$^{+/+}$ macrophages, whereas the levels of TLR4 transcripts in Cbl-b$^{-/-}$ macrophages before palmitate treatment were significantly lower than these in Cbl-b$^{+/+}$ macrophages (Fig. 3*F*). The levels of TLR4 gradually increased after palmitate treatment and reached the levels of Cbl-b$^{+/+}$ macrophages at 16 h (Fig. 3*F*).

Effects of Cbl-b overexpression on NF-κB and JNK signaling in RAW264.7 macrophages. We examined the effects of Cbl-b overexpresion on saturated FA-mediated expression of IL-6 in RAW264.7 macrophages. RAW264.7 macrophages transfected with the Cbl-b gene by lipofection expressed high amounts of Cbl-b protein, whereas the same cells transfected with the mock vector hardly expressed Cbl-b protein (Fig. 4*A*). As expected, overexpression of Cbl-b significantly suppressed palmitate-mediated IL-6 expression (Fig. 4*B*). The palmitate-induced changes in IκB phosphorylation and its protein level were suppressed by overexpression of Cbl-b in RAW264.7 macrophages (Fig. 4*C*). Palmitate stimulated IκB phosphorylation in mock vector-transfected RAW264.7 macrophages but gradually reduced its protein level. Overexpression of Cbl-b significantly suppressed palmitate-induced IκB phosphorylation and its degradation. Similarly, palmitate-induced JNK phosphorylation in mock vector-transfected RAW264.7 macrophages was canceled by overexpression of Cbl-b (Fig. 4*D*). These findings are consistent with the results shown in Fig. 3 and suggest that Cbl-b regulates saturated FA-mediated cytokine production in macrophages through the NF-κB and JNK signaling pathways.

Involvement of Cbl-b in TLR4-mediated saturated FA signaling. To address whether Cbl-b plays a role in TLR4-mediated saturated FA signaling, HEK293/TLR4 cells transfected with mock vector or HA-tagged Cbl-b were treated with palmitate and assessed by immunoblotting for degradation of V5-tagged TLR4 and Myc-tagged MyD88 (Fig. 5*A*). Saturated FAs induced degradation of TLR4, but not MyD88, in the presence of Cbl-b (Fig. 5*A*). Vehicle treatment did not change the amount of TLR4 or MyD88 (data not shown). On the basis of these results, we also examined Cbl-b–mediated ubiquitination of TLR4. At 3 h after palmitate treatment, immunoprecipitates of V5-tagged TLR4 from Cbl-b–transfected cells, using anti-V5 antibody, contained large amounts of ubiquitinated TLR4 compared with those from mock-transfected cells (Fig. 5*B*). Furthermore, epoxomicin, an inhibitor of the proteasome, significantly blocked palmitate-induced TLR4 degradation (Fig. 5*C*).

Because immunoprecipitation and immunoblot analysis using commercially available TLR4 antibodies did not detect TLR4 protein in Cbl-b$^{-/-}$ macrophages, flow cytometry was performed to assess TLR4 protein levels on the surface of macrophages. The TLR4 protein expression level on the surface of peritoneal macrophages was similar in Cbl-b$^{+/+}$ and Cbl-b$^{-/-}$ mice (Fig. 5*D*). Short-term (3-h) treatment with palmitate did not affect the expression of TLR4 (Fig. 3*D*) but significantly increased the TLR4 protein level on the surface of Cbl-b$^{-/-}$ macrophages. In contrast, the same treatment reduced the TLR4 protein level on the surface of Cbl-b$^{+/+}$ macrophages. However, palmitate treatment did not induce degradation of MyD88 and TRIF, even in Cbl-b$^{+/+}$ peritoneal macrophages (Fig. 5*E*). There were no differences in the protein levels of MyD88 and TRIF between Cbl-b$^{+/+}$ and Cbl-b$^{-/-}$ peritoneal macrophages (Fig. 5*E*). These results indicate that the effects of FA on TLR4 protein level on the surface of macrophages are mediated by Cbl-b–induced ubiquitination and degradation.

Induction of insulin resistance in Cbl-b$^{+/+}$ mice by Cbl-b$^{-/-}$ BMT. BMT was conducted to elucidate the importance of Cbl-b in the hematopoietic system. Bone marrow cells derived from Cbl-b$^{-/-}$ (Cbl-b$^{-/-}$ BMT) or Cbl-b$^{+/+}$ donors (Cbl-b$^{+/+}$ BMT) were transplanted into Cbl-b$^{+/+}$ recipient mice, followed by feeding the HFD to Cbl-b$^{-/-}$ BMT and Cbl-b$^{+/+}$ BMT mice for 24 weeks. We measured serum parameters, glucose tolerance, homeostasis model assessment of insulin resistance (HOMA-IR), and cytokine expression in the WAT of Cbl-b$^{+/+}$ and Cbl-b$^{-/-}$ BMT mice fed the HFD for 24 weeks. There were no differences in body composition and serum parameters between Cbl-b$^{+/+}$ and

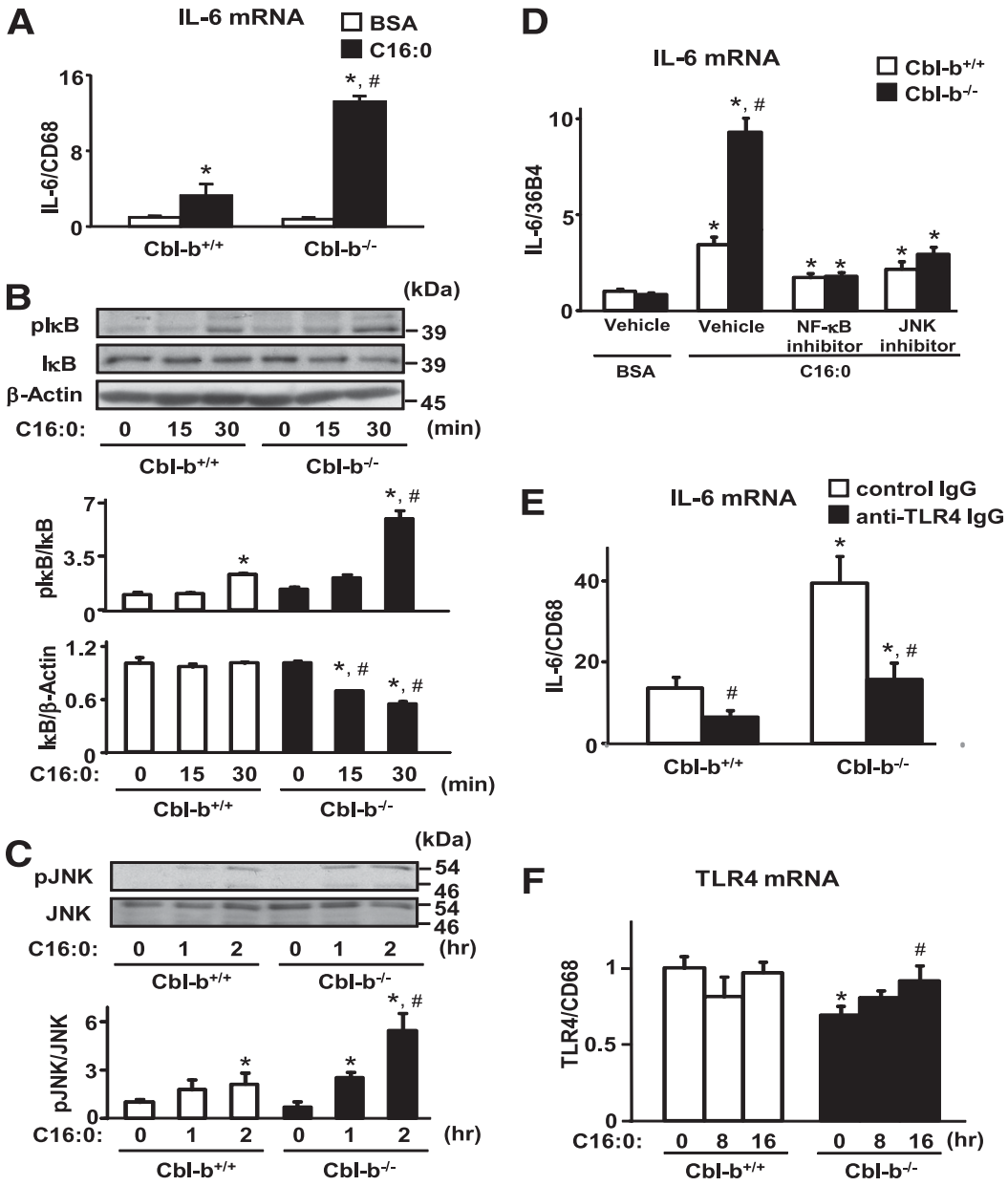

FIG. 3. Saturated FA-mediated NF-κB and JNK signaling in Cbl-b–deficient peritoneal macrophages. *A*: Peritoneal macrophages from 7- to- 9-week-old Cbl-b$^{+/+}$ and Cbl-b$^{-/-}$ mice were treated with palmitate (C16:0) for 16 h, and total RNA was extracted from these peritoneal macrophages. The amounts of IL-6 and CD68 (internal standard) transcripts were determined by real-time RT-PCR. Data are mean ± SD (n = 3). *P < 0.05 and #P < 0.05 compared with BSA- and palmitate-treated Cbl-b$^{+/+}$ peritoneal macrophages, respectively. *B* and *C*: Peritoneal macrophages from 7- to- 9-week-old Cbl-b$^{+/+}$ and Cbl-b$^{-/-}$ mice were treated with palmitate for the indicated time points. Whole-cell lysates were subjected to immunoblotting (20 μg/lane) using antibodies against the indicated proteins. The results are from three independent experiments. Data are densitometric ratios of phosphorylated IκB to total IκB, total IκB to β-actin, or phosphorylated JNK to total JNK and represent the mean ± SD values of three mice. *P < 0.05 and #P < 0.05 compared with time 0 and Cbl-b$^{+/+}$ peritoneal macrophages at the same time interval, respectively. *D*: Effects of IKK-2 inhibitor IV (500 nmol/L) or SP600125 (25 μmol/L) in DMSO (vehicle) on palmitate-induced IL-6 expression in Cbl-b$^{+/+}$ and Cbl-b$^{-/-}$ peritoneal macrophages estimated by the measurement of IL-6 expression. Peritoneal macrophages were pretreated with these chemical inhibitors for 2 h before palmitate treatment. Data are mean ± SD (n = 3). *P < 0.05 and #P < 0.05 compared with BSA with DMSO and Cbl-b$^{+/+}$ peritoneal macrophages, respectively. *E*: Effect of anti-TLR4/MD-2 IgG on palmitate-induced IL-6 mRNA expression in peritoneal macrophages was estimated by measuring IL-6 expression. Peritoneal macrophages were treated with anti-TLR4/MD-2 IgG or control IgG (18 μg/mL) for 2 h before treatment with palmitate. The amounts of IL-6 and CD68 (internal standard) transcripts were analyzed by real-time RT-PCR. Data are mean ± SD (n = 3). *P < 0.05 and #P < 0.05 compared with Cbl-b$^{+/+}$ peritoneal macrophages and control IgG treatment, respectively. *F*: Peritoneal macrophages were treated with palmitate for 8 or 16 h and subjected to total RNA extraction. The amounts of TLR4 and CD68 (internal standard) transcripts were assessed by real-time RT-PCR. Data are mean ± SD (n = 3). *P < 0.05 and #P < 0.05 compared with Cbl-b$^{+/+}$ peritoneal macrophages and Cbl-b$^{-/-}$ peritoneal macrophages without treatment with palmitate, respectively.

Cbl-b$^{-/-}$ BMT mice fed the HFD for 24 weeks (Table 1). Furthermore, there was no significant difference in body weight gains after 24 weeks of the HFD (Fig. 6*A*). Because the body weight and epididymal fat weight were similar to those of aged-matched, nonradiated standard mice, Cbl-b$^{-/-}$ BMT mice were not considered to be obese. Although both groups of recipient mice fed the HFD for 12 weeks after BMT showed normal responses on ITT, the response on ITT was disturbed in Cbl-b$^{-/-}$ BMT mice fed the HFD for 24 weeks (Fig. 6*B*). In addition, glucose

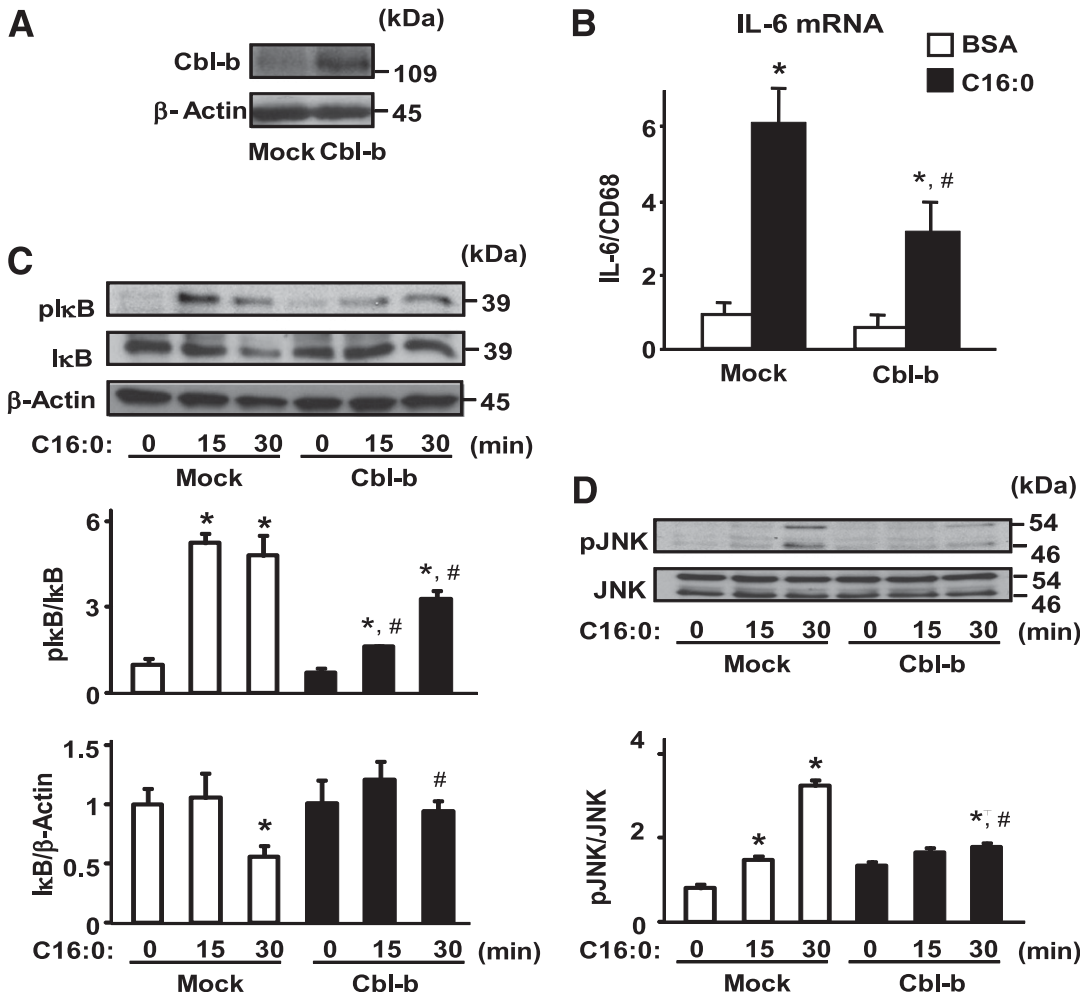

FIG. 4. Saturated FA-mediated NF-κB and JNK signaling in Cbl-b–overexpressing RAW264.7 macrophages. *A*: Whole-cell lysates (40 μg/lane) of RAW264.7 macrophages transfected with pCEFL (Mock) or pCEFL-Cbl-b-HA were subjected to immunoblotting. *B*: RAW264.7 cells transfected with mock vector or pCEFL-Cbl-b-HA were treated with 400 μmol/L BSA-conjugated palmitate for 16 h. The amounts of IL-6 and CD68 (internal standard) transcripts in these cells were analyzed by real-time RT-PCR. Data are mean ± SD (n = 3). *P < 0.05 and #P < 0.05 compared with BSA treatment and mock vector-transfected RAW264.7 cells, respectively. After treatment with palmitate to Cbl-b–overexpressing RAW264.7 macrophages for the indicated time intervals, whole-cell lysates (40 μg/lane) were subjected to immunoblotting for phosphorylated IκB, total IκB, and β-actin (*C*), and phosphorylated JNK and total JNK (*D*). Each experiment was independently reproduced three times. Data are densitometric ratios of phosphorylated IκB to total IκB, IκB to β-actin, and phosphorylated JNK to total JNK. Data are mean ± SD (n = 3). *P < 0.05 and #P < 0.05 compared with mock at 0 min and mock at the same time, respectively.

tolerance was exaggerated in Cbl-b$^{-/-}$ BMT mice compared with Cbl-b$^{+/+}$ BMT mice (Fig. 6*C*). However, there was no significant difference in HOMA-IR between the two groups (Fig. 6*D*). In addition, being fed the HFD for 24 weeks significantly increased the population of F4/80^{+}-CD11b^{+} macrophages in the WAT of Cbl-b$^{-/-}$ BMT mice compared with Cbl-b$^{+/+}$ BMT mice (Fig. 6*E*). Furthermore, IL-6 and MCP-1 expression levels in the WAT of Cbl-b$^{-/-}$ BMT mice were higher than those in the WAT of Cbl-b$^{+/+}$ BMT mice (Fig. 6*F*).

Inhibition of TLR4 signaling in obese Cbl-b$^{-/-}$ mice. To confirm the involvement of Cbl-b in TLR4-mediated saturated FA signaling in vivo, Cbl-b$^{+/+}$ and Cbl-b$^{-/-}$ mice fed the HFD for 5 weeks were intraperitoneally treated with Eritoran, a synthetic TLR4 antagonist. Eritoran did not change food intake, body weight, epididymal fat weight, or serum parameters, including blood glucose and serum insulin, of HFD-fed Cbl-b$^{+/+}$ and Cbl-b$^{-/-}$ mice (Table 1). Consistent with increased inflammation in the WAT of Cbl-b$^{-/-}$ mice, being fed the HFD for 5 weeks significantly increased fasting blood glucose and serum insulin levels in Cbl-b$^{-/-}$ mice (Fig. 7*A*). Interestingly, Eritoran significantly reduced fasting blood glucose and serum insulin levels in Cbl-b$^{-/-}$ mice fed the HFD compared with placebo (Fig. 7*A*). Consequently, Eritoran significantly improved the impaired HOMA-IR in Cbl-b$^{-/-}$ mice fed the HFD (Fig. 7*A*). These results indicate that Eritoran improved insulin resistance specifically observed in Cbl-b$^{-/-}$ mice fed the HFD. In addition, Eritoran significantly suppressed the HFD-induced increase in serum IL-6 levels of Cbl-b$^{-/-}$ mice (Fig. 7*B*). Histochemical analysis of WAT also showed that blockade of TLR4 resulted in inhibition of macrophage infiltration into WAT and reduced CLS formation by infiltrated macrophages (Fig. 7*C* and *D*). On the basis of our previous finding that MCP-1 is a critical chemokine that can induce macrophage infiltration into WAT (9), we also measured MCP-1 expression in WAT in the current study. MCP-1 expression was higher in the WAT of Cbl-b$^{-/-}$ mice than in Cbl-b$^{+/+}$ mice, and Eritoran treatment significantly suppressed the increased expression (Fig. 7*E*). As a result of

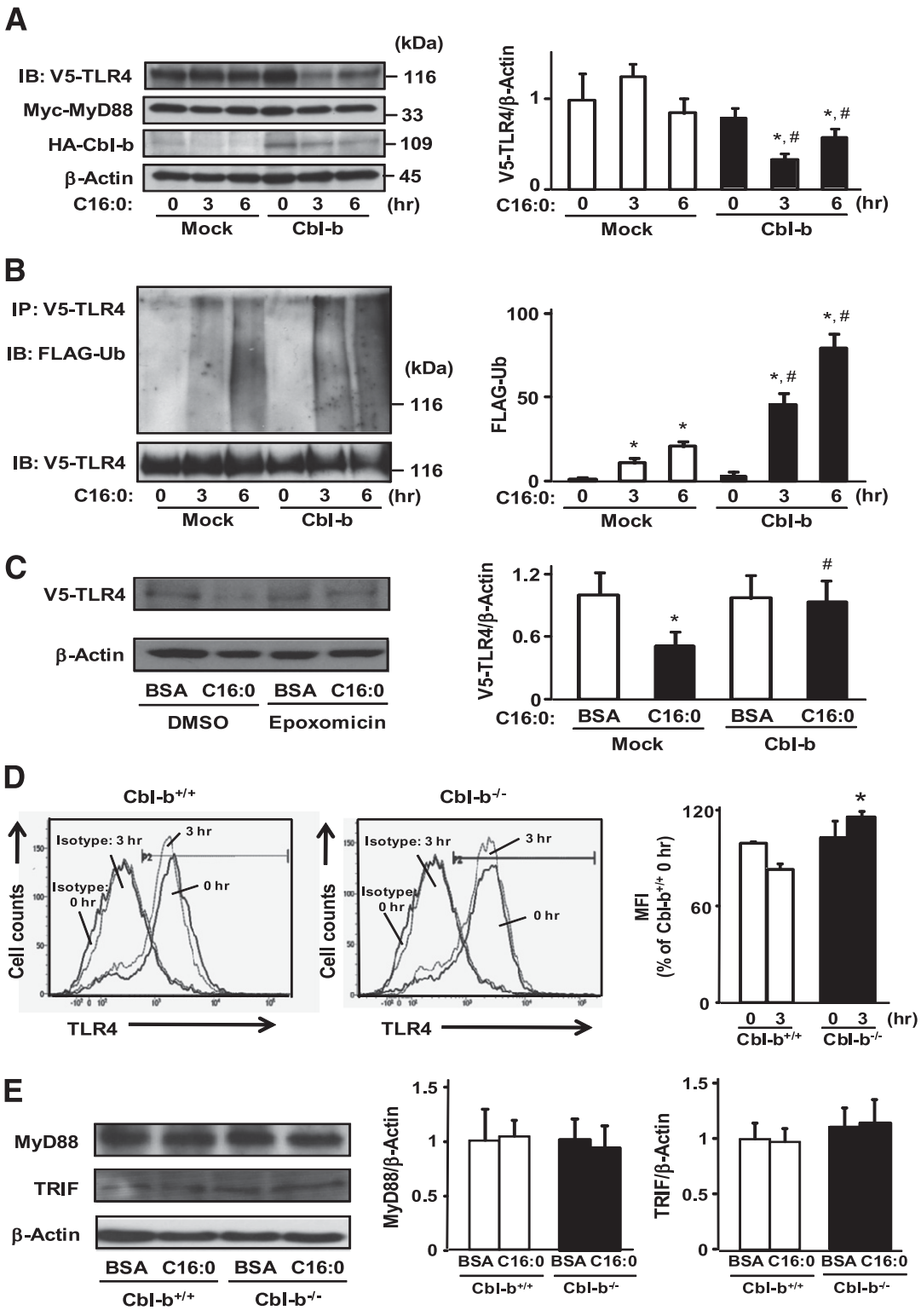

FIG. 5. Role of Cbl-b in TLR4-mediated saturated FA signaling. *A*: HEK293/TLR4 cells were transfected with TLR4-V5, MyD88-Myc, mock vector/pCEFL-Cbl-b-HA, and pcDNA3-FLAG-Ubiquitin. To analyze the degradation rates of saturated FA signaling molecules, these cells were treated with 100 μg/mL cycloheximide. After treatment with palmitate for the indicated time intervals, whole-cell lysates were subjected to immunoblotting (IB; 20 μg/lane) for the indicated proteins. Each experiment was independently reproduced three times. Data are densitometric ratio of V5 to β-actin and are mean ± SD values of three experiments. *$P < 0.05$ and #$P < 0.05$ compared with time 0 and mock at the same time interval, respectively. *B*: HEK293/TLR4 cells were transfected with TLR4-V5, MyD88-Myc, mock vector/pCEFL-Cbl-b-HA, and pcDNA3-FLAG-Ubiquitin. To analyze the ubiquitination of TLR4, MG132 was added to cells. After treatment with palmitate for the indicated time intervals, whole-cell lysates were immunoprecipitated (IP) with anti-V5 antibody. The immunoprecipitates were subjected to IB for the indicated proteins. Densitometric quantification of FLAG was performed with ImageJ software. Data are mean ± SD ($n = 3$). *$P < 0.05$ and #$P < 0.05$ compared with time 0 and mock at the same time interval, respectively. *C*: Effect of pretreatment with 100 nmol/L epoxomicin on palmitate-induced degradation of TLR4. HEK293/TLR4 cells were transfected with TLR4-V5, MyD88-Myc, pCEFL-Cbl-b-HA, and pcDNA3-FLAG-Ubiquitin. Cells were pretreated with epoxomicin for 3 h before palmitate treatment and then treated with palmitate for 3 h. Whole-cell lysates (20 μg/lane) were subjected to immunoblotting for the indicated proteins. Data are densitometric ratio of V5 to β-actin and are mean ± SD values of three experiments. *$P < 0.05$ and #$P < 0.05$ compared

these findings, we suggest that Eritoran reduces macrophage accumulation and CLS formation, at least in part, through the suppression of MCP-1 expression.

Long-term HFD feeding also induces obesity-associated insulin resistance, even in wild-type mice (5). Therefore, we tested whether Eritoran alters insulin resistance. The use of the HFD for 10 weeks induced hyperlipidemia and insulin resistance, even in wild-type mice (Supplementary Table 2 and Supplementary Fig. 4), whereas both pathological states were not noted in wild-type mice fed the HFD for 5 weeks (Table 1 and Fig. 7*A*). ITT results indicated that Eritoran treatment failed to improve the 10-week HFD-induced resistance in wild-type mice compared with placebo treatment (Supplementary Fig. 4). Eritoran also did not reduce HFD-induced accumulation of macrophages into the WAT in wild-type mice (data not shown), whereas feeding the HFD for 10 weeks resulted in accumulation of macrophages in the WAT in wild-type mice to an extent similar to that seen in wild-type mice fed the HFD for 18 weeks (Fig. 1*A*). In addition, Cbl-b expression in circulatory monocytes and immune cells, mainly macrophages, in the SV fraction, was not changed in wild-type mice (Supplementary Fig. 5).

DISCUSSION

Cbl-b functions as a negative regulator for activation of immune cells, such as lymphocytes and neutrophils, by ubiquitination of phosphatidylinositol 3-kinase and protein kinase C-θ (31,32). However, little information is available on the role of Cbl-b in the regulation of macrophages in contrast to its well-described roles in other immune cells (8,15,33,34). Interestingly, we found that palmitate treatment stimulated IL-6 expression in macrophages but not in lymphocytes or neutrophils (Supplementary Fig. 4). In this study, we investigated the function of Cbl-b in macrophages, especially as a negative regulator of FA-mediated cytokine expression in macrophages.

We reported previously that deficiency of the Cbl-b gene was associated with activation and recruitment of macrophages into WAT and caused peripheral insulin resistance in elderly mice (9), suggesting the involvement of Cbl-b in aging-induced insulin resistance. In addition to aging, obesity is another inducer of macrophage recruitment into WAT (4,5). To examine the relationship between saturated FAs and Cbl-b expression in macrophages, we treated peritoneal macrophages with palmitate. We found that palmitate treatment significantly downregulated Cbl-b expression in peritoneal macrophages and RAW264.7 cells at the protein and mRNA levels, respectively (Supplementary Fig. 4). Furthermore, increased saturated FAs can activate macrophages in WAT of Cbl-b$^{-/-}$ mice. Interestingly, recruitment of macrophages into WAT was noted in early stages of obesity in Cbl-b$^{-/-}$ mice. Moreover, insulin signaling was inhibited in insulin-sensitive organs of Cbl-b$^{-/-}$ mice fed the HFD compared with Cbl-b$^{+/+}$ mice. These findings suggest that HFD- and aging-induced recruitment of macrophages into WAT, as well as insulin resistance, are at least partly mediated by Cbl-b.

Downregulation of Cbl-b expression accentuates sepsis-related production of proinflammatory cytokines and chemokines in a model of polymicrobial acute pneumonia associated with TLR4 (15). Thus, Cbl-b can regulate the sepsis-induced TLR4-mediated acute inflammatory response. We report here that Cbl-b deficiency increased the expression of cytokines in macrophages induced by saturated FAs and that saturated FAs induced ubiquitination and degradation of TLR4 in the presence of Cbl-b. These findings suggest that Cbl-b negatively regulates saturated FA-mediated TLR4 signaling through ubiquitination of TLR4. Because Cbl-b recognizes the site of tyrosine phosphorylation in target protein receptors, followed by downregulation by ubiquitination (35), the recent evidence that LPS activates TLR4 through phosphorylation of ^{674}Tyr and ^{680}Tyr of human TLR4 (36) also supports our hypothesis. The current study also showed that saturated FAs served as ligands for TLR4 to induce the activation of NF-κB and JNK in Cbl-b$^{-/-}$ macrophages. This finding is consistent with the evidence that Cbl-b controls the link between TLR4 and intracellular adaptor MyD88 and regulates NF-κB cytokine signaling (15). In contrast, Han et al. (37) reported recently, both in vitro and in vivo, that Cbl-b negatively regulated LPS-induced TLR4 activation by ubiquitination and degradation of MyD88 and TRIF, but not TLR4. We found that palmitate treatment did not induce degradation of MyD88 and TRIF even in Cbl-b$^{+/+}$ peritoneal macrophages. FAs may induce TLR4 activation through a mechanism different from that of LPS. The reason for this discrepancy remains unknown. Further studies are necessary to elucidate such mechanism.

We used whole-body knockout mice of the Cbl-b gene in the current study. Therefore, we performed BMT to confirm the importance of Cbl-b in the hematopoietic system. The bone marrow-derived cells with specific depletion of Cbl-b gene exaggerated HFD-induced abnormalities on ITT and GTT, whereas a longer time after BMT elapsed before the infiltration of macrophages into the WAT of mice fed the HFD. Body weight was not different between mice transplanted with Cbl-b$^{+/+}$ and Cbl-b$^{-/-}$ bone marrow cells. Consistent with our findings, BMT of TLR4 gene-depleted cells did not induce changes in body weight but did ameliorate HFD-induced inflammation and insulin resistance in mice (19). In addition, palmitate-induced overexpression of IL-6 was noted only in macrophages, but not in lymphocytes or neutrophils (Fig. 3*B* and Supplementary Fig. 5). On the basis of these results, we suggest that Cbl-b plays a critical role in hematopoietic cells, especially in macrophages, in mice.

FA treatment preferentially downregulated the Cbl-b protein level in macrophages in vitro, leading to their activation. Interestingly, Cbl-b$^{-/-}$ BMT mice fed the HFD for 24 weeks showed disturbed responses in the ITT and GTT, accompanied by infiltration of macrophages into WAT, regardless of the nonobese status. Profound hyperlipidemia and insulin resistance without obesity were described recently in humans and in an animal model of lipodystrophy (38,39). Severe hyperlipidemia may induce activation and infiltration of macrophages into WAT,

with BSA with DMSO and C16:0 with DMSO, respectively. *D*: Peritoneal macrophages from Cbl-b$^{+/+}$ and Cbl-b$^{-/-}$ mice were cultured with 400 μmol/L palmitate, and cell surface TLR4 protein levels were determined by flow cytometry at the indicated time points. Samples were gated for F4/80^{+} and examined for TLR4 expression. Quantification of mean fluorescence intensity (MFI) of TLR4 expression was performed with Cell Quest Pro software. Data are mean ± SD (n = 3). *P < 0.05 compared with Cbl-b$^{+/+}$ macrophages treated with palmitate for 3 h. *E*: Peritoneal macrophages from Cbl-b$^{+/+}$ and Cbl-b$^{-/-}$ mice were treated with 400 μmol/L palmitate or vehicle (BSA) for 3 h. Whole-cell lysates (30 μg/lane) were subjected to immunoblotting for MyD88, TRIF, and β-actin. Data are densitometric ratio of MyD88 or TRIF to β-actin and are mean ± SD values of three experiments.

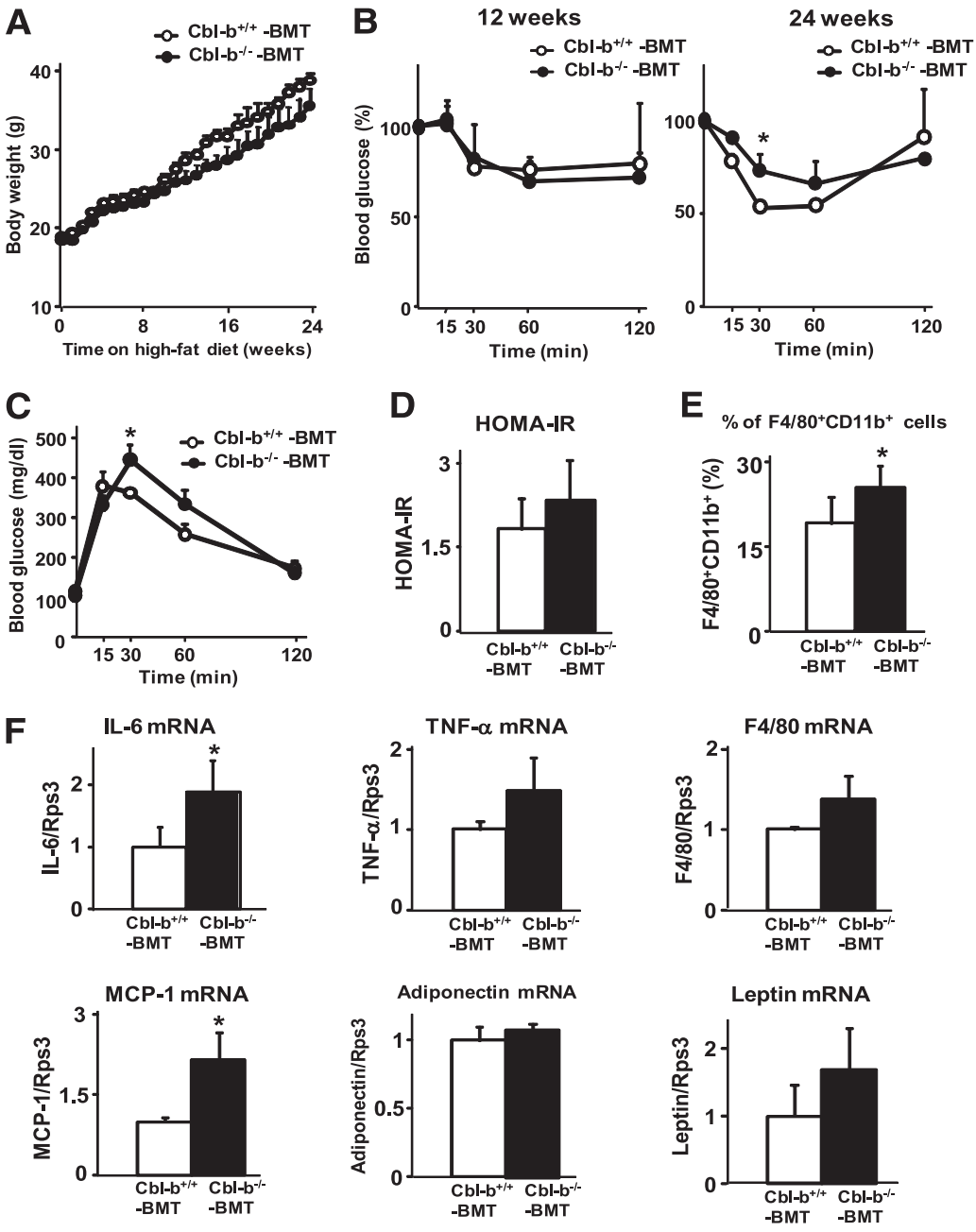

FIG. 6. Bone marrow-specific deletion of Cbl-b partially exaggerated long-term HFD-induced insulin resistance. *A*: Body weight of bone marrow-specific Cbl-b deficient (Cbl-b$^{-/-}$ BMT) and control (Cbl-b$^{+/+}$ BMT) recipient mice fed the HFD was monitored for 24 weeks. Data are mean ± SD (n = 7). *B*: Cbl-b$^{+/+}$ BMT and Cbl-b$^{-/-}$ BMT fed the HFD for 12 (*left panel*) or 24 weeks (*right panel*) were fasted for 12 h and then injected intraperitoneally with insulin at 0.75 mU/g body weight. Data are mean ± SD (12 weeks of HFD; Cbl-b$^{+/+}$ BMT, n = 5; Cbl-b$^{-/-}$ BMT, n = 6. 24 weeks of HFD; n = 3). *P < 0.05 compared with Cbl-b$^{+/+}$ BMT. *C*: Cbl-b$^{+/+}$ BMT and Cbl-b$^{-/-}$ BMT fed HFD for 23 weeks were fasted for 12 h and then injected intraperitoneally with glucose at 2 mg/g body weight. Data are mean ± SD (n = 3). *P < 0.05 compared with Cbl-b$^{+/+}$ BMT. *D*: HOMA-IR of Cbl-b$^{+/+}$ BMT and Cbl-b$^{-/-}$ BMT mice fed the HFD for 24 weeks was calculated. Data are mean ± SD (n = 3). *E*: WAT of Cbl-b$^{+/+}$ BMT and Cbl-b$^{-/-}$ BMT recipient mice fed the HFD for 24 weeks were subjected to flow cytometric analysis to determine the ratio of F4/80 and CD11b double-positive cells to total cells in stromal vascular fractions. Data are mean ± SD (Cbl-b$^{+/+}$ BMT, n = 6; Cbl-b$^{-/-}$ BMT, n = 5). *P < 0.05 compared with Cbl-b$^{+/+}$ BMT. *F*: The mRNA expression levels of IL-6, TNF-α, F4/80, MCP-1, adiponectin, and leptin in WAT of Cbl-b$^{+/+}$ BMT and Cbl-b$^{-/-}$ BMT fed the HFD for 24 weeks, measured by real-time RT-PCR. Data are mean ± SD (n = 3). *P < 0.05 compared with Cbl-b$^{+/+}$ BMT.

possibly through downregulation of Cbl-b levels. Obesity is not necessary for macrophage-mediated insulin resistance, although the HFD tends to induce obesity. However, the results from the BMT experiments could not exclude the possibility that the adiposity observed in Cbl-b$^{-/-}$ mice fed the HFD is associated with insulin resistance. Therefore, insulin resistance in Cbl-b$^{-/-}$ mice fed the HFD accompanied with adiposity was more apparent than that in Cbl-b$^{-/-}$ BMT mice fed the HFD. Further examination is necessary to elucidate this hypothesis.

Treatment with Eritoran failed to improve the 10-week HFD-induced resistance in wild-type mice (Supplementary Fig. 4). Feeding the HFD for 10 weeks did not change Cbl-b expression in circulatory monocytes and adipose tissue macrophages, although it induced hyperlipidemia in these mice (Supplementary Table 2 and Supplementary Fig. 5).

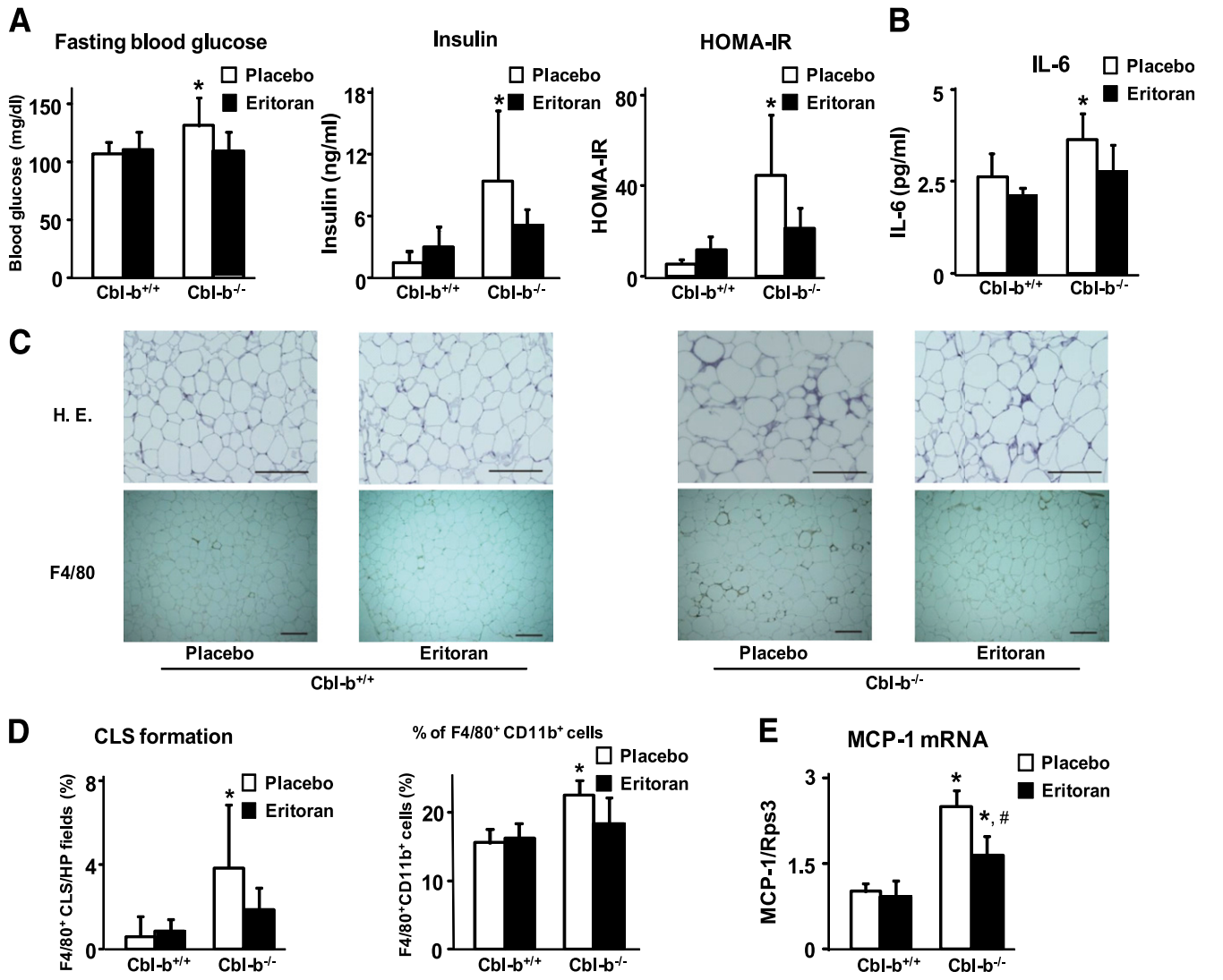

FIG. 7. Blockade of TLR4 by antagonist improved fasting blood glucose level and infiltration of macrophages into WAT in Cbl-b$^{-/-}$ mice. *A*: Cbl-b$^{+/+}$ and Cbl-b$^{-/-}$ mice fed the HFD for 5 weeks were injected intraperitoneally with Eritoran (4 mg/kg body weight) or placebo three times every 24 h, and fasting blood glucose, serum insulin, and HOMA-IR were measured. Data are mean ± SD (n = 4). *P < 0.05 compared with placebo-treated Cbl-b$^{+/+}$ mice. *B*: Concentrations are shown for serum IL-6 in Cbl-b$^{+/+}$ and Cbl-b$^{-/-}$ mice injected with Eritoran or placebo, measured by ELISA. Data are mean ± SD (n = 4). *P < 0.05 compared with placebo-treated Cbl-b$^{+/+}$ mice. *C*: The WAT of Cbl-b$^{+/+}$ or Cbl-b$^{-/-}$ mice administrated Eritoran or placebo were stained with hematoxylin and eosin and subjected to immunohistochemistry for F4/80, a macrophage marker. Scale bar = 200 μm. *D*: The number of CLS was counted in 15 separate high-power fields in seven slides per mouse. Data are mean ± SD (n = 3). The proportions of F4/80 and CD11b double-positive cells to total cells in SV fractions were measured by flow cytometric analysis. Data are mean ± SD (n = 3). *P < 0.05 compared with placebo-treated Cbl-b$^{+/+}$ mice. *E*: Expression of MCP-1 mRNA in WAT of Cbl-b$^{+/+}$ or Cbl-b$^{-/-}$ mice treated with Eritoran or placebo was measured by real-time RT-PCR. Data are mean ± SD (n = 3). *P < 0.05 and #P < 0.05 compared with placebo-treated Cbl-b$^{+/+}$ mice and Cbl-b$^{-/-}$ mice, respectively.

These findings indicate that feeding the HFD for 10 weeks does not activate TLR4 signaling in wild-type mice. Presumably, severe inflammation, such as macrophage activation associated with Cbl-b deficiency, did not occur in the WAT of wild-type mice fed the HFD for 10 weeks. These findings are consistent with the previous report that the initial stage of HFD-induced insulin resistance is independent of inflammation, whereas the more chronic state of insulin resistance is mediated by macrophage-induced proinflammatory action (40).

TLR4-deficient mice and C3H/HeJ mice, which carry a loss-of-function mutation in TLR4, are protected against HFD-induced insulin resistance and suppress saturated FAs-induced overexpression of cytokines (13,14,28). In this study, we examined the effect of a chemical analog, Eritoran, on insulin resistance and IL-6 expression in vivo. Eritoran is a structural analog of the lipid A portion of LPS and binds with TLR4 as an antagonist, and the crystal structure of Eritoran bound to the TLR4-MD2 complex has been described (18). Indeed, Eritoran inhibits LPS-induced TNF-α production in human whole blood samples (41). Interestingly, Eritoran inhibited the production of proinflammatory cytokines in macrophages stimulated by FA-induced TLR4 activation and also improved HFD-induced insulin resistance and the serum IL-6 level in Cbl-b$^{-/-}$ mice. In addition, we found that Eritoran treatment decreased CLS formation in WAT of Cbl-b$^{-/-}$ mice fed the HFD, at least in part, through reduction of MCP-1 expression in WAT. As described above, activation of Cbl-b–mediated ubiquitination of TLR4 is effective in inhibiting

obesity-induced expression of proinflammatory cytokines. Taken together, inhibition of TLR4 signaling by Eritoran or Cbl-b–mediated degradation seems an attractive therapeutic strategy for the treatment of obesity-related insulin resistance.

ACKNOWLEDGMENTS

This study was carried out as part of the Ground Research Announcement for Space Utilization, promoted by the Japan Aerospace Exploration Agency and the Japan Space Forum, to T.N. The study was supported by a grant-in-aid for scientific research from the Ministry of Education, Culture, Sports, Science, and Technology of Japan to T.N., Seed Production by the Japan Science and Technology Agency to T.N., and the Promotion of Basic Research Activities for Innovative Biosciences from the Bio-Oriented Technology Research Advancement Institution of Japan to T.N. This study was also partly supported by a high-technology research center grant from the Ministry of Education, Culture, Sports, Science, and Technology of Japan to the Juntendo University Research Institute for Disease of Old Ages, Tokyo, Japan.

No potential conflicts of interest relevant to this article were reported.

T.A. and K.H. designed the research; researched the data, including additional data for revision; and wrote the manuscript. S.Ka., S.Ko., A.Oc., K.U., A.S., and J.T. researched the data, including additional data for revision. A.Oh. and Y.M. contributed to the new analytic tools. S.T.-K. and Y.O. contributed to the new analytic tools and reviewed and edited the manuscript. M.O. and E.M.M. reviewed and edited the manuscript. T.N. designed the research, reviewed and edited the manuscript, and wrote the manuscript. T.N. is the guarantor of this work, and, as such, had full access to all the data in the study and takes responsibility for the integrity of the data and the accuracy of the data analysis.

The authors thank Stanley Lipkowitz (from the U.S. National Institutes of Health) for pCEFL-Cbl-b-HA, and Toshiaki Suzuki (from Tokyo Metropolitan Institute of Medical Science) for pcDNA3-FLAG-Ubiquitin, and are grateful to Hua Gu (from University of Columbia) and Tetsuya Inazu (from University of Ritsumeikan) for providing Cbl-b$^{-/-}$ mice. The authors thank Eisai Research Institute for providing E5564.

REFERENCES

1. Hotamisligil GS. Inflammation and metabolic disorders. Nature 2006;444:860–867
2. Shoelson SE, Lee J, Goldfine AB. Inflammation and insulin resistance. J Clin Invest 2006;116:1793–1801
3. Hotamisligil GS, Shargill NS, Spiegelman BM. Adipose expression of tumor necrosis factor-alpha: direct role in obesity-linked insulin resistance. Science 1993;259:87–91
4. Weisberg SP, McCann D, Desai M, Rosenbaum M, Leibel RL, Ferrante AW Jr. Obesity is associated with macrophage accumulation in adipose tissue. J Clin Invest 2003;112:1796–1808
5. Xu H, Barnes GT, Yang Q, et al. Chronic inflammation in fat plays a crucial role in the development of obesity-related insulin resistance. J Clin Invest 2003;112:1821–1830
6. de Luca C, Olefsky JM. Stressed out about obesity and insulin resistance. Nat Med 2006;12:41–42; discussion 42
7. Keane MM, Rivero-Lezcano OM, Mitchell JA, Robbins KC, Lipkowitz S. Cloning and characterization of cbl-b: a SH3 binding protein with homology to the c-cbl proto-oncogene. Oncogene 1995;10:2367–2377
8. Liu YC, Gu H. Cbl and Cbl-b in T-cell regulation. Trends Immunol 2002;23:140–143
9. Hirasaka K, Kohno S, Goto J, et al. Deficiency of cbl-b gene enhances infiltration and activation of macrophages in adipose tissue and causes peripheral insulin resistance in mice. Diabetes 2007;56:2511–5122.
10. Suganami T, Nishida J, Ogawa Y. A paracrine loop between adipocytes and macrophages aggravates inflammatory changes: role of free fatty acids and tumor necrosis factor alpha. Arterioscler Thromb Vasc Biol 2005;25:2062–2068
11. Wellen KE, Hotamisligil GS. Inflammation, stress, and diabetes. J Clin Invest 2005;115:1111–1119
12. Lee JY, Ye J, Gao Z, et al. Reciprocal modulation of Toll-like receptor-4 signaling pathways involving MyD88 and phosphatidylinositol 3-kinase/AKT by saturated and polyunsaturated fatty acids. J Biol Chem 2003;278:37041–37051
13. Shi H, Kokoeva MV, Inouye K, Tzameli I, Yin H, Flier JS. TLR4 links innate immunity and fatty acid-induced insulin resistance. J Clin Invest 2006;116:3015–3025
14. Tsukumo DM, Carvalho-Filho MA, Carvalheira JB, et al. Loss-of-function mutation in Toll-like receptor 4 prevents diet-induced obesity and insulin resistance. Diabetes 2007;56:1986–1998.
15. Bachmaier K, Toya S, Gao X, et al. E3 ubiquitin ligase Cblb regulates the acute inflammatory response underlying lung injury. Nat Med 2007;13:920–926
16. Chiang YJ, Kole HK, Brown K, et al. Cbl-b regulates the CD28 dependence of T-cell activation. Nature 2000;403:216–220
17. Nakao R, Hirasaka K, Goto J, et al. Ubiquitin ligase Cbl-b is a negative regulator for insulin-like growth factor 1 signaling during muscle atrophy caused by unloading. Mol Cell Biol 2009;29:4798–4811
18. Kim HM, Park BS, Kim JI, et al. Crystal structure of the TLR4-MD-2 complex with bound endotoxin antagonist Eritoran. Cell 2007;130:906–917
19. Saberi M, Woods NB, de Luca C, et al. Hematopoietic cell-specific deletion of toll-like receptor 4 ameliorates hepatic and adipose tissue insulin resistance in high-fat-fed mice. Cell Metab 2009;10:419–429
20. Hirasaka K, Nikawa T, Yuge L, et al. Clinorotation prevents differentiation of rat myoblastic L6 cells in association with reduced NF-kappa B signaling. Biochim Biophys Acta 2005;1743:130–140
21. Ogawa T, Furochi H, Mameoka M, et al. Ubiquitin ligase gene expression in healthy volunteers with 20-day bedrest. Muscle Nerve 2006;34:463–469
22. Noble JE, Bailey MJ. Quantitation of protein. Methods Enzymol 2009;463:73–95
23. Spayd RW, Bruschi B, Burdick BA, et al. Multilayer film elements for clinical analysis: applications to representative chemical determinations. Clin Chem 1978;24:1343–1350
24. Shimizu S, Yasui K, Tani Y, Yamada H. Acyl-CoA oxidase from *Candida tropicalis*. Biochem Biophys Res Commun 1979;91:108–113
25. Minami A, Iseki M, Kishi K, et al. Increased insulin sensitivity and hypoinsulinemia in APS knockout mice. Diabetes 2003;52:2657–2665
26. Senn JJ, Klover PJ, Nowak IA, et al. Suppressor of cytokine signaling-3 (SOCS-3), a potential mediator of interleukin-6-dependent insulin resistance in hepatocytes. J Biol Chem 2003;278:13740–13746
27. Solinas G, Vilcu C, Neels JG, et al. JNK1 in hematopoietically derived cells contributes to diet-induced inflammation and insulin resistance without affecting obesity. Cell Metab 2007;6:386–397
28. Suganami T, Tanimoto-Koyama K, Nishida J, et al. Role of the Toll-like receptor 4/NF-kappaB pathway in saturated fatty acid-induced inflammatory changes in the interaction between adipocytes and macrophages. Arterioscler Thromb Vasc Biol 2007;27:84–91
29. Kanarek N, Ben-Neriah Y. Regulation of NF-κB by ubiquitination and degradation of the IκBs. Immunol Rev 2012;246:77–94
30. Akashi S, Shimazu R, Ogata H, et al. Cutting edge: cell surface expression and lipopolysaccharide signaling via the toll-like receptor 4-MD-2 complex on mouse peritoneal macrophages. J Immunol 2000;164:3471–3475
31. Fang D, Wang HY, Fang N, Altman Y, Elly C, Liu YC. Cbl-b, a RING-type E3 ubiquitin ligase, targets phosphatidylinositol 3-kinase for ubiquitination in T cells. J Biol Chem 2001;276:4872–4878
32. Gruber T, Hermann-Kleiter N, Hinterleitner R, et al. PKC-theta modulates the strength of T cell responses by targeting Cbl-b for ubiquitination and degradation. Sci Signal 2009;2:ra30
33. Qiao G, Li Z, Molinero L, et al. T-cell receptor-induced NF-kappaB activation is negatively regulated by E3 ubiquitin ligase Cbl-b. Mol Cell Biol 2008;28:2470–2480
34. Gustin SE, Thien CB, Langdon WY. Cbl-b is a negative regulator of inflammatory cytokines produced by IgE-activated mast cells. J Immunol 2006;177:5980–5989
35. Dikic I, Giordano S. Negative receptor signalling. Curr Opin Cell Biol 2003;15:128–135

36. Medvedev AE, Piao W, Shoenfelt J, et al. Role of TLR4 tyrosine phosphorylation in signal transduction and endotoxin tolerance. J Biol Chem 2007;282:16042–16053
37. Han C, Jin J, Xu S, Liu H, Li N, Cao X. Integrin CD11b negatively regulates TLR-triggered inflammatory responses by activating Syk and promoting degradation of MyD88 and TRIF via Cbl-b. Nat Immunol 2010;11:734–742
38. Huang-Doran I, Sleigh A, Rochford JJ, O'Rahilly S, Savage DB. Lipodystrophy: metabolic insights from a rare disorder. J Endocrinol 2010;207:245–255
39. Herrero L, Shapiro H, Nayer A, Lee J, Shoelson SE. Inflammation and adipose tissue macrophages in lipodystrophic mice. Proc Natl Acad Sci U S A 2010;107:240–245
40. Lee YS, Li P, Huh JY, et al. Inflammation is necessary for long-term but not short-term high-fat diet-induced insulin resistance. Diabetes 2011;60:2474–2483
41. Mullarkey M, Rose JR, Bristol J, et al. Inhibition of endotoxin response by e5564, a novel Toll-like receptor 4-directed endotoxin antagonist. J Pharmacol Exp Ther 2003;304:1093–1102